Size-tunable synthesis of stable superparamagnetic iron oxide nanoparticles for potential biomedical applications

Faquan Yu,[1,2] Victor C. Yang[1,3]

[1]Department of Pharmaceutical Sciences, College of Pharmacy, The University of Michigan, 428 Church Street, Ann Arbor, Michigan 48109-1065

[2]Key Laboratory for Green Chemical Process of Ministry of Education, Wuhan Institute of Technology, Wuhan 430073, China

[3]Tianjin Key Laboratory for Modern Drug Delivery and High Efficiency, Tianjin University, Tianjin 300072, China

Abstract: Dextran-coated superparamagnetic nanoparticles (MNPs) have widespread biomedical applications. The superparamagnetic behavior, specifically regulated size, and smooth morphology are crucial requirements for essentially all of these applications. Presented herein is an innovative double-coating strategy that would allow for a size-controlled synthesis of MNPs. Small monocrystalline iron oxide nanoparticles (MIONs) were first synthesized, which served as the source of superparamagnetic properties. These MIONs were then treated in an acetate buffer containing biocompatible dextran polymer. Under such an environment, the colloidal MIONs would be quickly agglomerated by the acetate ions, and the formed coalescent body of MION would then be stabilized simultaneously by coating with dextran. By regulating the MION or dextran concentration as well as the thermal incubation time, the sizes of these first formed nanoparticles (termed 1st-NPs) could be readily controlled. A second dextran coating step was further applied to smoothen the 1st-NPs in attaining a final product (termed 2nd-NPs). The 2nd-NPs exhibited robust storage stability because of the additional coating shell. Results successfully confirmed the plausibility of this approach, as these MNPs displayed not only a smooth outline and a narrow size distribution but also the essential superparamagnetic behavior and a significantly prolonged stability on storage. © 2009 Wiley Periodicals, Inc. J Biomed Mater Res 92A: 1468–1475, 2010

Key words: superparamagnetic nanoparticle; size regulation; stable storage; double coating

INTRODUCTION

Iron oxide-based magnetic nanoparticles (MNPs) have attracted great interest owing to their widespread applications in biomedicine including sensing,[1] cell labeling,[2] imaging,[3] targeted delivery of drugs[4] and genes,[5] as well as localized therapeutic hyperthermia.[6] Several comprehensive reviews concerning the properties, syntheses, and applications can be found in the literature.[7–9] Generally speaking, these MNPs comprise a magnetic core consisting of magnetite (Fe_3O_4) or maghemite (Fe_2O_3), which is surrounded by a coating of a biocompatible polymer such as dextran or starch. Although the monocrystalline iron oxide nanoparticles (MIONs) serve as the superparamagnetic resource, the polymer coating prevents MNPs from aggregation because of the intrinsic magnetic attraction. In addition, the activatable functional groups (e.g. $-NH_2$, $-OH$) on the polymer also allow for conjugation of bioactive compounds such as drugs or antibodies on the MNP surface for subsequent targeting and delivery purposes.

The diameter of the MION core and the overall hydrodynamic size of MNPs (i.e. MION plus the polymer shell) are both of critical significance with regard to *in vivo* applications. Although nanoparticles greater than 300 nm in size are known to be sequestered in liver and spleen and removed by the mononuclear phagocyte system, particles less than 10 nm in diameter become small enough for rapid clearance through extravasations and renal filtration.[10,11] Indeed, MNPs with size ranging between 100 and 200 nm in diameter have been reported to possess a long-

circulating plasma half-life for imaging and targeting[12] via the so-called enhanced permeability and retention (EPR) phenomenon of the tumor.[13] In contrast, it has been demonstrated that magnetic properties such as magnetic-induced targeting of nanoscale magnetic particles depend primarily on the magnetophoretic mobility; a parameter that is enhanced solely when increasing the size of the magnetic core.[14]

Thus far, strategies for MNP synthesis include: (1) *in situ* synthesis of MION in the presence of polymer[15]; (2) *in situ* synthesis of polymer in the presence of premade MION[16]; or (3) direct mixing of presynthesized MION with polymer together.[17] However, some of these strategies involve the use of a surfactant as emulsifying agent, which is often not biocompatible and also affects the efficiency for subsequent surface modification with bioactive agents. Most critically, most of these strategies normally yielded an ill-defined morphology and an irregular size distribution for the produced MNPs and lacked the control of size.

Presented herein is an innovative and facile double-coating approach that allows for preparing MNPs with smooth morphology and desirable size control, and yet comprising of a large core structure with high-magnetophoretic mobility while retaining the essential superparamagnetic behavior for biomedical applications. As reported, the monocrystalline iron oxide nanoparticles (i.e. MIONs; the primary constituent of the magnetic core) are stable without forming tightly associated aggregates in acidic medium.[18] Our previous experiments showed that this stability of MION can also be alternatively attained by coating MIONs with a biocompatible polymer such as dextran and that, in contrast, the colloidal MION suspension tends to agglomerate in the presence of acetate ions. Therefore, the underlying hypothesis is that if MION is treated in an acetate buffer containing dextran, both the processes of forming a coalescent body of MION and stabilizing this large magnetic core by dextran can take place *in situ* and simultaneously. By manipulating the MION or dextran concentrations in the solution, and/or by altering the pH or thermal incubation time of the reaction, a tightly size-controlled structure of MION can be realized. To further smoothen the morphology, these first-coated nanoparticles (termed 1st-NPs) are coated for a second time with a dextran solution (nanoparticles thus prepared are termed as 2nd-NPs). A schematic illustration of this approach is demonstrated in Figure 1. Results successfully confirmed the plausibility of the approach, as the double-coated magnetic nanoparticles not only display a smooth morphology and size but also exhibit the essential superparamagnetic behavior and a significantly enhanced stability during storage.
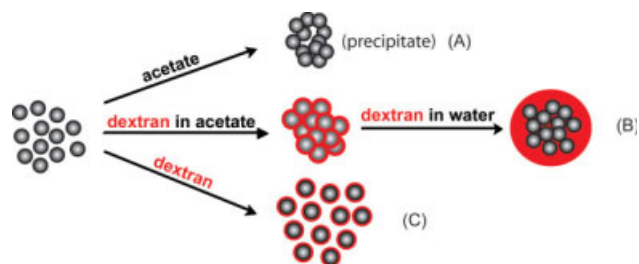

Figure 1. Schematic illustration of the proposed double-coating strategy: (A) precipitation of MION by acetate buffer only; (B) nanoparticles obtained after treatment with acetate buffer containing dextran (1st-NPs), and after second coating with a dextran solution (2nd-NPs); (C) MIONs coated with dextran solution only. [Color figure can be viewed in the online issue, which is available at www.interscience.wiley.com.]

EXPERIMENTAL

Materials

Dextran (from Leuconostoc mesenteroides, MW: 9000–11,000), ferrous chloride tetrahydrate ($FeCl_2 \cdot 4H_2O$), ferric chloride hexahydrate ($FeCl_3 \cdot 6H_2O$), HCl, and sodium hydroxide were purchased from Sigma-Aldrich Chemical Co. Water was distilled and deionized (ddH_2O).

Preparation of the superparamagnetic, monocrystalline iron oxide nanoparticles

MION was synthesized according to a modified procedure of Kim et al.[19] Briefly, a solution containing 0.76 mol/L of ferric chloride and 0.4 mol/L of ferrous chloride (molar ratio of ferric to ferrous was ~2:1) was prepared at pH 1.7 under N_2 protection. The iron solution was then added dropwise into a 1.5M NaOH solution under vigorous mechanical stirring. The reaction mixture was gradually heated (1°C/min) to 78°C and held at this temperature for 1 h under stirring and N_2 protection. After separation of the supernatant by using a permanent magnet, the wet sol was treated with 0.01M HCl and then sonicated for 1 h. The acidified colloidal suspension of MION was filtered through a 0.45 μm and then a 0.22 μm membrane, followed by condensing to a suspension containing ~34 mg Fe/mL using a Millipore (USA) ultrafiltration unit.

Preparation of double-coated magnetic nanoparticles

To synthesize 1st-NPs, dextran was predissolved into a pH4 acetate buffer solution. To 3 mL of this solution, 1 mL of the MION suspension prepared above (pH = 4) was added all at once under vigorous agitation. The mixture was then incubated in a 78°C water bath. To regulate the size of the produced nanoparticles, various concentrations of dextran and MION as well as different incubation time

TABLE I
**Summary of Experimental Conditions and Size Distributions Following Syntheses
of the 1st-NP and 2nd-NP Products**

	Dextran Concentration in the First Coating (mg/mL)	MION Concentration (mg (Fe)/mL)	Incubation Time (min)	Size of 1st-NP (nm)	Size of 2nd-NP (nm)
1	380	34	25	188.1 ± 11.8	195.6 ± 15.8
2	380	25	25	139.5 ± 8.7	152.7 ± 13.0
3	380	15	25	79.7 ± 6.2	94.0 ± 9.1
4	320	25	25	187.2 ± 13.1	190.1 ± 11.4
5	320	15	25	96.4 ± 8.9	107.7 ± 8.7
6	380	15	35	112.1 ± 7.8	116.1 ± 8.0
7	380	15	45	125.5 ± 8.8	142.2 ± 11.3
8	380	15	55	152.9 ± 9.2	158.7 ± 12.8

Both the concentrations of dextran and MION were before mixing; the ratio of dextran over MION was fixed at 3/1 in volume.

were attempted. The resulting 1st-NPs were purified twice by using a permanent magnet separator.

To prepare the final MNP product (i.e. the 2nd-NPs) possessing a smooth morphology and particle size, 1 mL of the above-synthesized 1st-NPs (15 mg Fe/mL) was added into 3 mL of a dextran aqueous solution (320 mg/mL) under agitation. After incubating the solution at 78°C for 15 min, the final product was separated using a magnetic separator.

Characterization

Morphology was examined by transmission electron microscopy (TEM) using a JEOL 3011 high-resolution electron microscope (JEOL, Tokyo, Japan) operated at an accelerated voltage of 300 kv. Samples were prepared by placing diluted particle suspensions on formvar film-coated copper grids (01813-F, Ted Pella, USA) and then dried at room temperature. Particle size was measured by a NICOMP 380 ZLS dynamic light scattering (DLS) instrument (PSS, Santa Barbara, CA) using the 632 nm line of a HeNe laser as the incident light. The NICOMP software was employed to analyze the volume-averaged size. Polymer contents of both the 1st-NPs and 2nd-NPs were determined by a Q50 thermogravimetric analyzer (TGA; TA Instruments, USA) under N_2 atmosphere at a temperature increase rate of 20°C/min from 30 to 600°C. Superparamagnetic properties were assessed at 25°C by using a superconducting quantum interference device (SQUID) (Quantum Design, San Diego, CA). Iron contents of the magnetic nanoparticles were measured by means of the inductively coupled plasma-optical emission spectroscopy (ICP-OES) analysis using the Perkin–Elmer Optima 2000 DV device (Perkin–Elmer, Boston, MA). Stability was examined by DLS in terms of the variation in particle size versus time, after suspending MNPs into 0.1M PBS solution at room temperature. FTIR was performed on lyophilized samples after they were compressed into ~1-mm thick discs with spectroscopic grade KBr.

RESULTS

Figure 1(B) illustrated the two-step process of producing the MION-based, dextran-coated MNPs. As

seen, bare MIONs were first synthesized as the building blocks of the magnetic core. The 1st-NPs were then generated by suspending the colloidal bare MIONs into an acetate buffer containing dextran, followed by heating the mixture at 78°C for a certain period of time. After obtaining the 1st-NPs, the ultimate 2nd-NPs were produced by further coating and heating the 1st-NPs in a freshly prepared suspending medium containing dextran only.

Results summarized in Table I indicated that particle sizes of the 1st-NPs could be regulated by altering several parameters during the first coating step, including dextran and MION concentration as well as the thermal incubation time. When pairing data in samples #2 and #4 or samples #3 and #5 together for comparison (see Table I), it was obvious that under the same MION concentration (i.e. either 25 or 15 mg Fe/mL) and incubation time (25 min), reducing dextran concentration resulted in an increase of the size of the 1st-NPs. A modest reduction in dextran concentration from 380 to 320 mg/mL led to a relatively significant change in particle size (from 139.5 nm and 79.7 nm in sample #2 and #3 to 187.2 nm and 96.4 nm in sample #4 and #5, respectively). Conversely, when dextran concentration and incubation time were held constant with MION concentration being reduced by a scale of ~10 mg Fe/mL, such as those seen in samples #1 through #3 and #4 to #5, a dramatic decrease in particle size was observed. Alternatively, by holding both dextran and MION concentration in the reaction mixture unchanged but elevating the incubation time (samples 3# and #6 through #8) also appeared to enhance particle growth of the 1st-NPs. Because the main purpose of the second dextran coating was to smoothen the surface morphology and stabilize the MNPs from aggregation by magnetic attraction, there was no major difference in particle size between the 1st-NPs and 2nd-NPs.

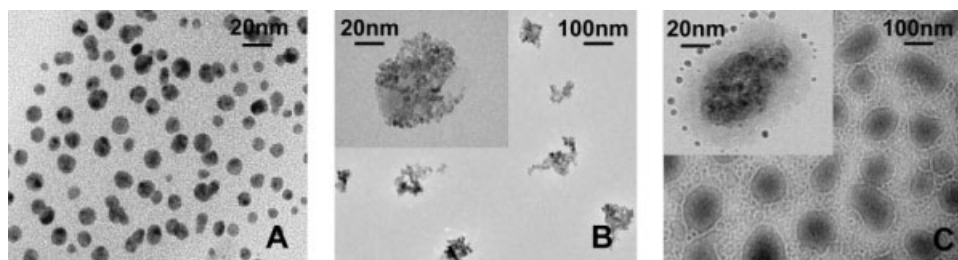TEM images of the synthesized MNPs were presented in Figure 2. The bare MION product dis-

Figure 2. Transmission electron microscopy (TEM) images of (A) MIONs; (B) 1st-NPs; and (C) 2nd-NPs (i.e. final). Both the images of B and C corresponded to 2# in Table I.

played a homogeneous dispersion with a size distribution of 9 ± 1.9 nm, as calculated from the TEM image [Fig. 2(A)]. As anticipated, acetate ions induced coagulation of the mono-dispersed, colloidal iron oxide particles, as clusters of MION sols were observed for the 1st-NPs [Fig. 2(B)]. Besides its stabilization effect in preventing particles from precipitation, the adhesive dextran polymer appeared to also act as a cross-linking agent to connect the small MIONs to form the large clusters of magnetic core structures. Apparently, dextran was not present in sufficient amount during the first coating process to fix the morphological appearance of these particles, as both the shape and outline of these 1st-NPs were rather irregular. Indeed, dextran coating could only be observed vaguely, when the TEM image of the particle was carried out at a much higher magnification [see insert in Fig. 2(B)]. Nonetheless, following an additional dextran coating on the 1st-NPs, the 2nd-NPs exhibited smooth outline with tightly controlled size [Fig. 2(C)]. Unlike the first step of MNP preparation, the second coating event occurred primarily on the particle surface, as dextran polymer could be easily identified by TEM under a high magnification [see insert in Fig. 2(C)]. Besides, there are some satellite-like small particles within the 2nd-MNP. These small particles, however, were supposed to be largely removed during the washing process. The remaining amount of small particles, whether by volume or by weight, was low compared with the whole MNP. There was slight probability of retaining some of the uncoated MIONs, although it is difficult to identify the coating shell in the TEM image, simply because the positively charged MIONs were exposed to a high concentration of the negative-charged dextran solution. In other words, the outmost layer of the 2nd-NP was virtually all of dextran, without the presence of naked MION. The observed good stability of the 2nd-NP, shown later, was actually attributed to the thick and complete dextran coating shell.

Measurements using a thermogravimetric analyzer (TGA) of the polymer contents of these synthesized MNPs also gave consistent results. As shown by the

data in Figure 3, the 1st-NPs yielded a 10.01% weight loss using bare MIONs as the standard (i.e. 100% weight remaining). Obviously, this weight loss was primarily attributed to the introduction of dextran to bare MIONs during synthesis of the 1st-NPs. As expected, the 2nd-NPs displayed a total weight loss of 17.30%, 7.29% more than that of the 1st-NPs, because of the incorporation of additional dextran polymer to the previously coated nanoparticles.

Figure 4 demonstrated the stability of the synthesized MNPs. Although there was an abrupt elevation of size in the 1st-NP suspension after 2 h of incubation in PBS solution (pH 7.4) at room temperature, the 2nd-NP suspension remained virtually stable during the entire course of storage of 120 h under the same experimental conditions.

The magnetic properties of MIONs and 2nd-NPs were also examined by SQUID, and the results were shown in Figure 5. Both MION and the 2nd-NP exhibited a typical superparamagnetic behavior in which particles did not remain magnetized in the absence of an external magnetic field, as reflected by
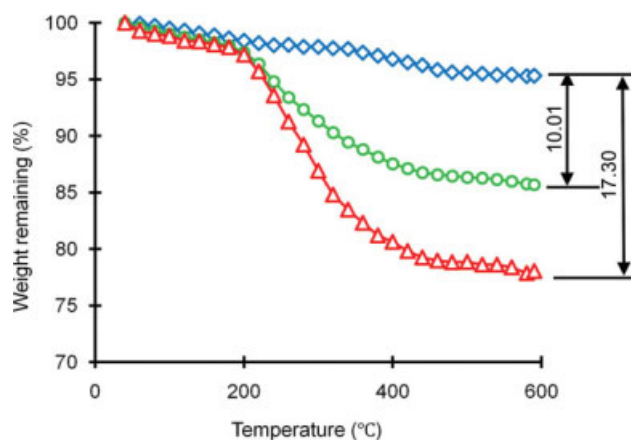

Figure 3. Thermogravimetric analysis (TGA) curves of MIONs (top), 1st-NPs (middle), and 2nd-NPs (bottom) obtained at a temperature increase rate of 20°C/min from 30 to 600°C under nitrogen atmosphere. The 1st-NPs and 2nd-NPs corresponded to 2# in Table I. [Color figure can be viewed in the online issue, which is available at www.interscience.wiley.com.]
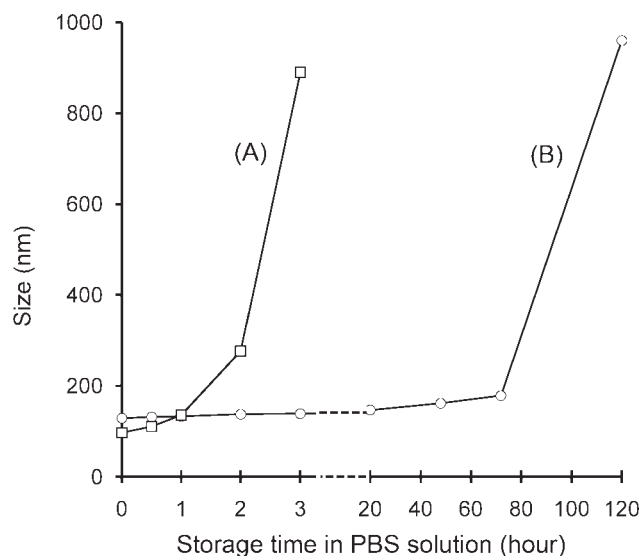
Figure 4. Stability of the 1st-NPs (A) and 2nd-NPs (B) corresponding to 2# in Table I, stored in PBS solution (0.1M, pH = 7.4).

the overlap between the magnetization and demagnetization curves and absence of a hysteresis loop. In addition, the 2nd-NP preparation displayed a saturation magnetic moment of 89.1 emu/g(Fe) that was in close resemblance with that (93.2 emu/g(Fe)) of the native MION without dextran coating.

DISCUSSION

Existing dextran-coated superparamagnetic nanoparticles were generally synthesized by coprecipitation of ferrous and ferric salts in a dextran solution in the presence of a strong base such as NaOH or NH$_4$OH. Although this strategy of forming dextran-coated nanoparticles was completed in single step, it nevertheless lacked the capability and flexibility to regulate the size and morphology of the final product. To overcome such shortcomings, a facile and robust approach that included a sequence of three individual and independent procedures was developed. The first step was to synthesize small diameter monocrystalline iron oxide nanoparticles (MIONs) possessing the superparamagnetic behavior that was essential for the majority of biomedical applications. As being recognized, MION remained stable without forming aggregates in the HCl solution (pH 4). This was because MION carried abundant superficial hydroxyl groups that were protonated (Fe—OH$_2^+$) in acidic medium to produce positive surface charges, thereby preventing them from coagulation. Increasing pH, MION will lose its positive superficial charge and eventually aggregate and precipitate. Coincidently, the isoelectric point (PI) of MION was

experimentally determined to be around 6.4 and its zeta potential in a pH4 HCl solution was ~+25.4 mV.[20–22] The purpose of this independent synthesis of MION was that it would allow for an open choice of conditions for subsequent polymer coating and size control.

The second step, termed first coating because it involved coating MION with dextran in the existence of acetate ions, was primarily for size regulation. As reported, the colloidal MION was easily surface-modified by certain carboxylate-containing compounds (R—COO$^-$) including dimercaptosuccinate, citrate, and tartarate.[23,24] However, the MION suspension precipitated when reacting with acetate. This phenomenon, in major part, was because of the reaction between superficial hydroxyl groups on MION (Fe—OH) and carboxylate ions to form Fe—O—C(O)—R linkages, a similar procedure as in literature,[23,24] which was herein testified by FTIR, as shown in Figure 6. A new absorbance peak at 1404 cm^{-1}, which corresponded to the symmetric vibration of the C—O bond, was identified when comparing the FTIR spectra with that of MION alone. The new formatoin of the linkage dramatically subtracted the stability effect stemming from the superficial hydroxyl groups. In addition, hydration of acetate ions and hence their ability to separate water molecules from the lyophilic MION according to the Hofmeister rule[25] was another cause of the precipitating power of acetate ions on MION. In contrast,
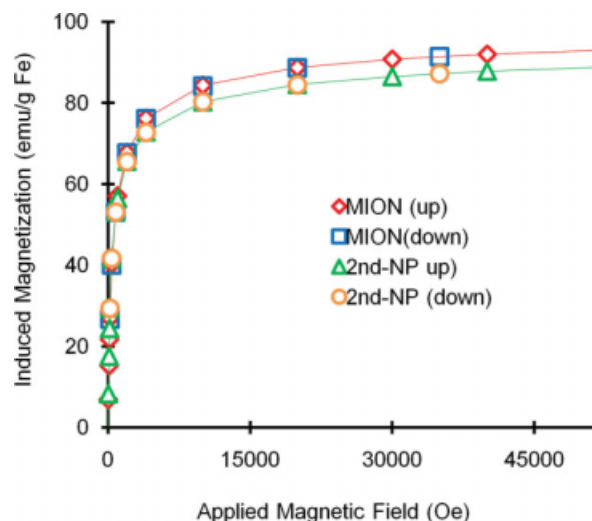

Figure 5. Magnitization/demagnitization curves of MION (top) and 2nd-NP (bottom) by SQUID at 25°C. The 2nd-NP was the sample of 2# in Table I. No hysteresis loop was observed in either curve, indicating the presence of superparamagnetic behavior for both MION and the double-coated product (i.e. 2nd-NPs). Both types of nanoparticles also displayed a similar leverage of saturation magnetization (Ms), as reflected by almost overlapped plateaus. [Color figure can be viewed in the online issue, which is available at www.interscience.wiley.com.]
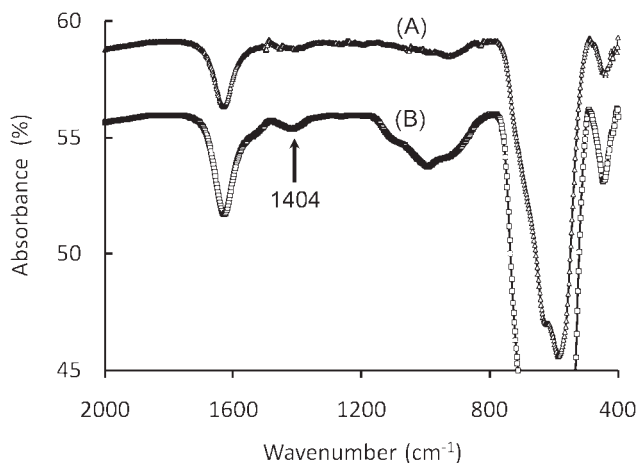
Figure 6. FTIR spectrum of MION (A) and the acetate-treated MION (B). The acetate-treated MION displayed an extra peak at 1404 cm^{-1}, which attributed to the symmetric vibration of C—O from the Fe—O—C(O) —R linkage between MION and acetate ions.

iron-oxide-based magnetic nanoparticles were often stabilized by coating with a dextran polymer via hydrogen bonds formed between the hydroxyl groups on both MION and dextran. Owing to the small size and high-surface area-to-volume of MION, this coating is normally strong and independent of pH. On the basis of such existing knowledge, we hypothesized that if MION is treated in an acetate buffer containing dextran, then both of the processes of MION aggregation and dextran coating can take place *in situ* and simultaneously. This concomitant occurrence of acetate-induced coagulation and dextran-induced separation of the coalescent MION would offer the unique benefit of regulating the particle size of the produced MNPs, as formation of the final product relies on the competition of two reaction kinetics; that is, MION aggregation and dextran coating. For instance, if the aggregation rate is slow as opposed to the rate of coating, such as under the situation of the presence of a high concentration of dextran in the acetate buffer, then only small dextran-coated particles would be produced. A signified example of this case would be when MIONs were coated in a dextran solution containing no acetate ions, whereas in theory and practice, only monocrystalline structures of iron oxide particles would be formed [see Fig. 1(C)]. Conversely, if aggregation takes place quickly when the coating rate is slow, such as by increasing the MION or acetate concentrations or reducing the dextran concentration in the coating medium, then formation of large MNPs would be expected. Similar to the extreme case displayed in Figure 1(A), MION would precipitate quickly as a large mass in acetate buffer containing no dextran. Furthermore, enhanced heating of the

reaction mixture would augment the kinetic energy of the nanoparticles, thereby accelerating their collision rates and facilitating MION aggregation. Results presented in Table I have successfully confirmed our hypotheses, and by manipulating experimental parameters such MION or dextran concentrations in the reaction mixture as well as the thermal incubation time periods, MNPs with controllable sizes can be readily produced.

Although this simultaneous aggregation/coating tactic was capable of regulating the size of the produced nanoparticles, TEM image in Figure 2(B) still indicated that the 1st-NPs were nevertheless irregular in morphology. Experimentally, the 1st-NPs demonstrated poor stability in PBS buffer. It should be noted that the 1st-NP preparation in many ways, such as the irregular configurations, closely resembled to most of the commercial products (e.g. fliudMAG-CMX; Chemicell, German), except that the size distribution of our MNPs was more narrower than those of existing commercial products; a tribute to this newly developed coating strategy. To prevail over these hurdles, a second coating process that paved an extra layer of dextran on the surface of 1st-NPs was adopted. As shown in Figure 2(C), this additional dextran rendered the surfaces of the final MNPs notably smooth. More importantly, surface dextran provides a shielding effect on the surface energy of these colloidal nanoparticles, thereby preventing them from aggregation during storage. As demonstrated from results in Figure 4, the stability of the 1st-NPs was boosted ~50-fold by this second dextran coating, from a period of 2 h to greater than 100 h. Furthermore, the thick shell of dextran on the surface allows nanoparticles to be loosely associated via weak van der Waals forces, therefore remaining in a fluffy conglomerate state after sedimentation and suitable for redispersion, without encountering the so-called "caking" event (i.e. by forming a compact cake of tightly bound aggregates) even after long-term storage in an aqueous medium (data not shown).

For *in vivo* applications of magnetic nanoparticles, such as magnetic targeting and MRI, superparamagnetic behavior is of paramount importance. As from its definition, individual particles with superparamagnetic property do not maintain intrinsic magnetization in the absence of an external magnetic field, and therefore, they will not agglomerate in solution before administration because of lack of magnetic attraction between particles. However, MION will only exhibit superparamagentic behavior below certain size threshold, namely the size of a single magnetic domain. The domain size for MION has been determined to be below 15 nm.[26–29] In contrast, the efficiency of magnetic-mediated interaction such as targeting depends primarily on the magnetophoretic

mobility; a parameter that can be enhanced only by increasing the size of the magnetic core. To this regard, the described technology of coalescing and coating MION simultaneously offers another significant benefit. Although the exceedingly thin layer of dextran between MION crystals would provide a shielding effect to maintain the individual crystals under their original size of a single magnetic domain (size of bare MION was 9 ± 1.9 nm) thereby retaining the superparamagnetic behavior, the coexistence of acetate ions rendered MIONs to flocculate or, in other words, to form loosely associated fluffy conglomerates with large magnetic cores thereby retaining necessary magnetophoretic mobility for biomedical applications. Results in Figure 5 confirmed the former event (i.e. superparamagnetism), whereas TEM findings in Figure 2(C) revealed the latter phenomenon (i.e. large core of MION).

Overall, the described double-coating strategy in preparing MNPs offers a number of advantages over currently existing methods. First, it allows for the synthesis of MNPs with tailored size and smoothened configuration. As discussed previously, the size and morphology are of paramount significance with regard to clinical applications of these MNPs. To dodge the removal by RES and clearance by the kidney and liver systems thereby yielding a long blood circulating lifetime, it is essential to control the size of nanoparticles to be around 100–200 nm. In addition, these physical attributes also dictate the pharmacokinetics and biodistribution of MNPs under *in vivo* situations. Secondly, MNPs synthesized by means of this new method not only retain the superparamagentic behavior of MION that is essential for virtually all clinical applications but also maintain a large core structure of MION that is highly responsive to attraction by the external magnetic field employed during MRI and tumor targeting. Thirdly, the markedly prolonged stability on storage greatly facilitates the suitability of these MNPs for biomedical applications. Last but not least, the simplicity and flexibility of this new methodology permit MION to be coated with virtually all types of biocompatible polymers containing different functional groups, thereby enabling surfaces of these MNPs to be further modified with various recognition moieties (e.g. antibodies) or bioactive ligands (e.g. the RGD peptide) for targeting. To this regard, the value of this new coating strategy is prevalent and widespread.

Dr. Victor C. Yang is currently a Chang Kang Scholar by the Chinese Ministry of Education at the School of Chemical Engineering, Tianjin University, Tianjin, China 300072.

References

1. Osaka T, Matsunaga T, Nakanishi T, Arakaki A, Niwa D, Iida H. Synthesis of magnetic nanoparticles and their application to bioassays. Anal Bioanal Chem 2006;384:593–600.
2. Wilhelm C, Billotey C, Roger J, Pons JN, Bacri J-C, Gazeau F. Intracellular uptake of anionic superparamagnetic nanoparticles as a function of their surface coating. Biomaterials 2003;24:1001–1011.
3. Thorek DL, Chen AK, Czupryna J, Tsourkas A. Superparamagnetic iron oxide nanoparticle probes for molecular imaging. Ann Biomed Eng 2006;34:23–38.
4. Cheng J, Teply BA, Jeong SY, Yim CH, Ho D, Sherifi I, Jon S, Farokhzad OC, Khademhosseini A, Langer RS. Magnetically responsive polymeric microparticles for oral delivery of protein drugs. Pharm Res 2006;23:557–564.
5. Dobson J. Gene therapy progress and prospects: Magnetic nanoparticle-based gene delivery. Gene Ther 2006;13:283–287.
6. Matteucci ML, Anyarambhatla G, Rosner G, Azuma C, Fisher PE, Dewhirst MW, Needham D, Thrall DE. Hyperthermia increases accumulation of technetium-99m-labeled liposomes in feline sarcomas. Clin Cancer Res 2000;6:3748–3755.
7. Mornet S, Vasseur S, Grasset F, Duguet E. Magnetic nanoparticle design for medical diagnosis and therapy. J Mater Chem 2004;14:2161–2175.
8. Neuberger T, Schopf B, Hofmann H, Hofmann M, von Rechenberg B. Superparamagnetic nanoparticles for biomedical applications: Possibilities and limitations of a new drug delivery system. J Magn Magn Mater 2005;293:483–496.
9. Gubin SP, Koksharov YA, Khomutov GB, Yurkov GY. Magnetic nanoparticles: Preparation, structure and properties. Russian Chem Rev 2005;74:489–520.
10. Sachdeva MS. Drug targeting systems for cancer therapy. Expert Opin Invest Drug 1998;7:1849–1864.
11. Gaur U, Sahoo SK, De TK, Ghosh PC, Maitra A, Ghosh PK. Biodistribution of fluoresceinated dextran using novel nanoparticles evading reticuloendothelial system. Int J Pharm 2000;202:1–10.
12. Enochs WS, Harsh G, Hochberg F, Weissleder R. Improved delineation of human brain tumors on MR images using a long-circulating, superparamagnetic iron oxide agent. J Magn Reson Imaging 1999;9:228–232.
13. Maeda H, Wu J, Sawa T, Matsumura Y, Hori K. Tumor vascular permeability and the EPR effect in macromolecular therapeutics: A review. J Control Release 2000;65:271–284.
14. Pekas N, Granger M, Tondra M, Popple A, Porter MD. Magnetic particle diverter in an integrated microfluidic format. J Magn Magn Mater 2005;293:584–588.
15. Molday RS. US Patent 4 452 773, 1984.
16. Ramirez LP, Landfester K. Magnetic polystyrene nanoparticles with a high magnetite content obtained by miniemulsion processes. Macromol Chem Phys 2003;204:22–31.
17. Landfester K, Ramirez LP. Encapsulated agnetite particles for biomedical application. J Phys-Condens Mater 2003;15:S1345–S1361.
18. Campos AFC, Tourinho FA, da Silva GJ, Lara MCFL, Depeyrot J. Nanoparticles superficial density of charge in electric double-layered magnetic fluid: A conductimetric and potentiometric approach. Eur Phys J E 2001;6:29–35.
19. Kim DK, Zhang Y, Voit W, Rao KV, Muhammed M. Synthesis and characterization of surfactant-coated superparamagnetic monodispersed iron oxide nanoparticles. J Magn Magn Mater 2001;225:30–36.
20. Fauconnier N, Bee A, Roger J, Pons JN. Synthesis of aqueous magnetic liquids by surface complexation of maghemite nanoparticles. J Mol Liq 1999;83:233–242.
21. Sousa MH, Rubim JC, Sobrinho PG, Tourinho FA. Biocompatible magnetic fluid precursors based on aspartic and glutamic

acid modified maghemite nanostructures. J Magn Magn Mater 2001;225:67–72.

22. Hingston FJ, Atkinson RJ, Posner AM, Quirk JP. Specific adsorption of anions. Nature 1967;215:1459–1461.

23. Fauconnier N, Pons JN, Roger J, Bee A. Thiolation of maghemite nanoparticles by dimercaptosuccinic acid. J Colloid Interface Sci 1997;194:427–433.

24. Fauconnier N, Bee A, Massart R, Dardoize F. Direct determination of organic acids in a ferrofluid (γ-Fe$_2$O$_3$) by high-performance liquid chromatography. J Liq Chromatogr 1996;19:783–797.

25. Martin A. Colloids. In: Martin A, editior. Physical Pharmacy, 4th ed. Philadelphia, PA: Lea & Febiger; 1993. p 393–422.

26. Jeong U, Teng X, Wang Y, Yang H, Xia Y. Superparamagnetic colloids: Controlled synthesis and niche applications. Adv Mater 2007;19:33–60.

27. Tartaj P, Morales M, Veintemillas-Verdaguer S, Gonzalez-Carreno T, Serna CJ. The preparation of magnetic nanoparticles for applications in biomedicine. J Phys D: Appl Phys 2003;36:R182–R197.

28. Frenkel J, Doefman J. Spontaneous and induced magnetisation in ferromagnetic bodies. Nature 1930;126:274–275.

29. Gupta AK, Gupta M. Synthesis and surface engineering of iron oxide nanoparticles for biomedical applications. Biomaterials 2005;26:3995–4021.